European Conference on Computational Fluid Dynamics
ECCOMAS CFD 2006
P. Wesseling, E. Oñate, J. Périaux (Eds)

AERODYNAMIC SHAPE OPTIMIZATION USING DISCRETE ADJOINT FOMULATION BASED ON OVERSET MESH TECHNIQUE

B.J. Lee* and Chongam Kim†

*Seoul National University, School of Mechanical & Aerospace Engineering,
e-mail: mecha777@hitel.net
Web page: http://mana.snu.ac.kr/

† Seoul National University, School of Mechanical & Aerospace Engineering
e-mail: chongam@snu.ac.kr

Key words: Discrete Adjoint Variable Method, Overset Approach, Optimal Shape Design, B-Spline, S-BIG (Spline-Boundary Intersecting Grid)

Abstract. *A new design approach for a delicate treatment of complex geometries such as wing/body configuration is arranged using overset mesh technique under large scale computing environment. For the in-depth study of the flow physics and highly accurate design, several special overlapped structured blocks such as collar grid, tip-cap grid, and etc. which are commonly used in refined drag prediction are adopted to consider the applicability of the design code to practical problems. Various pre- and post-processing techniques for overset flow analysis and sensitivity analysis are devised or implemented to adapt overset mesh technique to the design optimization problem based on Gradient Based Optimization Method (GBOM). In the pre-processing, the convergence characteristics of the flow solver and sensitivity analysis are improved by overlap optimization method. Moreover, a new post-processing method, Spline-Boundary Intersecting Grid (S-BIG) scheme, is proposed by considering the ratio of cell area for more refined prediction of aerodynamic coefficients and convenient evaluation of sensitivities under parallel computing environment. For the sensitivity analysis, adjoint formulations for overset boundary conditions are implemented into the existing fully hand-differentiated sensitivity analysis code. A smooth geometric modification on the overlapped surface boundaries and evaluation of analytic grid sensitivities can be performed by Spline patch and mapping from physical grids to the patched Spline function. Careful design works for the drag minimization problem of DLR-F4 are performed using the newly-developed and -applied techniques. And the design results from conventional design problem demonstrate the capability of the present design approach successfully.*

1 INTRODUCTION

In aerodynamic shape optimization (ASO) for aircraft, GBOM (Gradient Based Optimization Method) is generally used because it is very efficient method to find optimum

shape and it can be easily applied to the MDO frameworks. Typical GBOM consists of four elements: Flow solver, sensitivity analysis code, grid generator (or grid modifier), and optimization algorithm. Before completing the design tools, an accurate and efficient flow solver is required for the computation of pressure distribution and aerodynamic loads such as lift, drag and pitching moment that compose the objective functions to be optimized. As the computational environment rapidly develops, the interests of CFD are focused on large-scale computations over complex geometries.[1, 2] Keeping pace with these trends, various grid techniques are used in the flow analyses and design optimization problems over complex geometries.

The design problem of multiple body aircraft geometries have been a matter of concern since late 1990s. Design method using multi-block system doesn't require any additional new techniques by comparing single block problems. Therefore as a straightforward extension of single block case, multi block system is easily applied to design of wing/body configurations and full body supersonic aircraft by numerous researchers.[3-5] Multi-block grid technique can secure a good grid quality. However, in case of moving grid or deforming grid applications, severe grid changes or even the grid topology changes are inevitable and these works cannot be performed fully automatically under multi-block environment. On the other hand, in case of unstructured grid system, the automatic mesh deformation can be easy work. In this reason, unstructured discrete adjoint variable codes are developed by, Nielsen(1998)[6], Kim(2000)[7] Jameson(2001)[8] et al. Nevertheless, compared with the structured grid, far more grid points are needed to analyze the flow in keeping the same resolution of solution. And additionally, it requires much more memory and computational time cost than the structured grid does even with the same number of grid points.

In view of these issues, the overset grid technique has several benefits to be applied to the large scale flow analysis and design optimization problems. At first, the grid topology is relatively simple to represent the deforming grid. Secondly, the movement of the grids, the change of the part position, and the exchange of parts is easily implemented. On the third, high-resolved flow solutions can be obtained through a relatively small number of grid points. Finally, the fully automatic grid-generations are possible because of the simple grid topology. These characteristics of overset mesh technique can derive the design optimization to the final goal, '*fully automatic aerodynamic design from CAD models*'. Development of adjoint variable codes based on overset mesh system is performed by only a few researchers. Multi-element airfoil with hand-differentiation of two-equation turbulence model is performed by Kim et al.[9] In case of three-dimensional problem a simple turbine vane design is carried out by Liau et al. They applied continuous adjoint approach for Euler-equations using implicit hole-cutting method to the design work.[10]

In the present paper, we applied several major pre- and post-processing methods for overset mesh system to aerodynamic shape design based on discrete adjoint approach. These techniques are newly devised or adapted for sensitivity analysis and design problem. Thus, sub-cell transfinite interpolation[11] for treatment of the orphan cells which are generated on the overlapped surface region in case of N-S calculation, Spline-Boundary Interpolation Grid(S-BIG) scheme for easy calculation of cell differentiation, and the overlap optimization[12] for high quality flow analysis results and good convergence characteristics of adjoint variable

code are resolved in the design optimization tools for complex geometries. Exploiting these techniques a drag minimization problem for DLR-F4 wing/body configurations in the overset grid system composed of typical 4 component blocks and 3 box blocks are carried out. [13]

2 NUMRICAL TECHNIQUES

2.1 Overlap Optimization for Adjoint Variable Code

As mentioned above main focus of the present work is on the application of adjoint variable method in discrete approach to the complex overset mesh system. Recently there are many progresses in flow analysis techniques for overset mesh system. The main issues of the overset flow analysis codes are focused upon the preprocessors such as PEGSUS[12], DCF3D[14], Beggar[15], Overture[16] and etc. These are high quality overset preprocessors. Especially, PEGASUS is one of the most efficient and robust code and a tremendous number of applications, i.e., flow analyses of very complex geometries as like full body aircraft, space craft, turbine blade, and so on, are carried out using this code in NASA. In these applications, the number of blocks is too much and the block connectivity of grid systems is inevitably so complicated to resolve the complicated flow phenomena with refined definition of analysis. As a result, an automatic finding process for hole-searching and construction of block connectivity are applied to the latest version. This technique is named by overlap optimization. This method can improve the convergence characteristics of overset analysis code by considering the ratio of cell volume or cell aspect ratio of donor and fringe cells. In addition, it can diminish the oscillation of the overset solution by minimizing overlapped different computation region in one physical space. The present sensitivity analysis code is definitely affected by the oscillation of the overset solution, too. Therefore the convergence characteristics of adjoint variable code cannot be secured without the overlap optimization. The convergence characteristics for adjoint variable code with and without overlap optimization are compared in Fig. 1. This figure shows that manual hole-cutting and donor finding routines cannot secure stable convergence of the adjoint variable code. For more details about overlap optimization process, refer to Ref.[12].

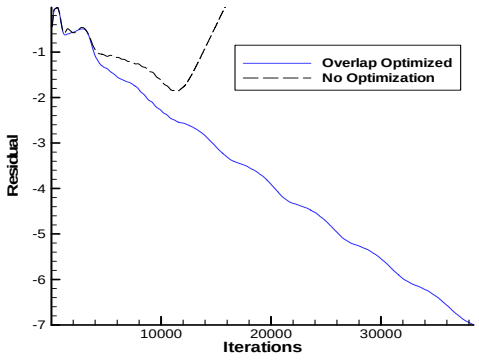

Fig. 1. Residual History of Overlap Optimized Overset Adjoint Code

2.2 Spline-Boundary Intersecting Grid (S-BIG) Scheme

2.2.1. Main Cell Reformation

In case of post processor for overset flow analysis, Zipper grid scheme[17] is widely used in calculation of aerodynamic coefficients. Zipper grid is a kind of grid reconstruction method. This method consists of blanking process of overlapped region and reconstruction process with an unstructured surface grid set. The flow variables on the zipper grid are interpolated from donor cells of computational overlapped blocks around the same physical point. However, the flux differential terms from arbitrary number of donor cells make it difficult to apply this method to adjoint variable code. In the present work, a newly devised Spline-Boundary Intersecting Grid (S-BIG) scheme is applied to the post processing routine and sensitivity analysis to make the differentiation process easy. The objective of S-BIG is preparation of evaluating routines for aerodynamic coefficients that require no interpolation process from donor cells. Assuming that Zipper grid scheme is reconstruction of grids on the level of a block, S-BIG is reconstitution of grids on the level of a cell. Thus arbitrary number of information transferal between blocks, which makes difficulties in differentiation of objective functions, is not necessary because this method does not requires except the boundary information to reform surface grid cell.

S-BIG scheme is composed by 4 stages. On the first stage, boundaries of the overlapped surface are determined by user. In case of the interface between fuselage and collar block, the outer boundary of the collar grid is chosen as shown in Fig. 2. The interfaces on wing surface such as collar-wing, wing-tipcap boundaries can be specified by a constant line(*y=constant*). And the determined boundaries can be parameterized by B-Spline function.

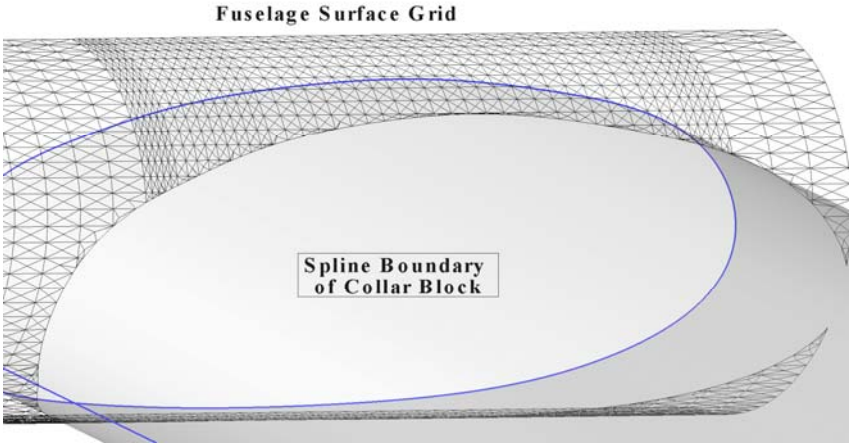

Fig. 2. Spline boundary of collar block at the interface with fuselage surface.

The next process is dividing the surface grid points into inner and outer vertices based on the Spline boundary. The outer vertices are set as normal vertices (NBLAK=1) and the inner as blanked vertices (NBLANK=0) as like hole cutting process as shown in Fig. 3-(a). Then there are 16 cases for inner and outer vertex distribution on a surface cell as shown in Fig. 3-(b). The surface cells are classified by 3 kinds of cells as like conservative Chimera scheme.[18] They are named by normal cell, cut cell, blanked cell and this classification is given in Fig.3.

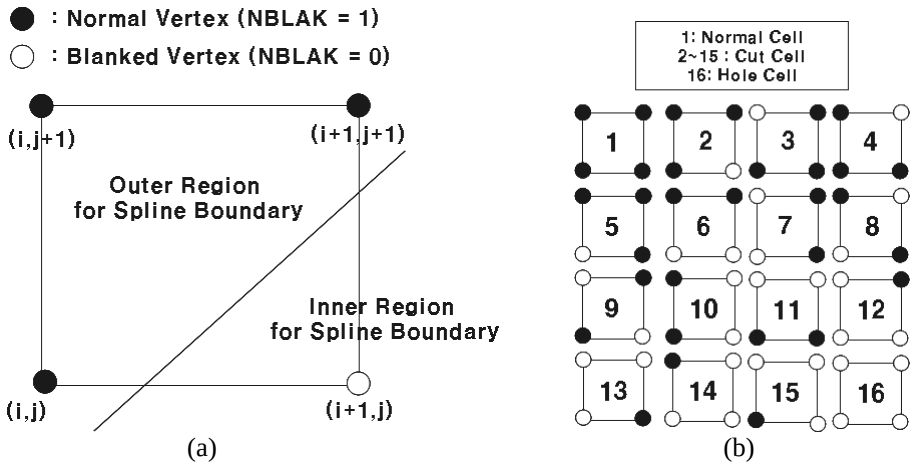

Fig. 3. (a) Blanking process by spline boundary (b) Classification of blanked surface cells

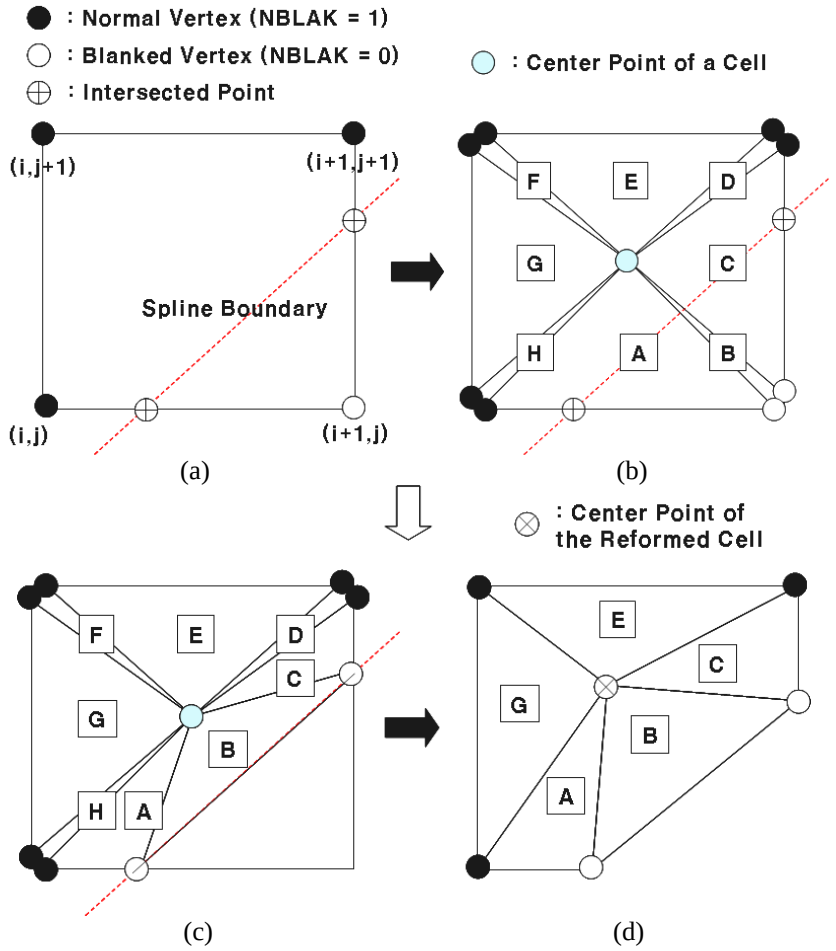

Fig. 4. Reconstruction of cut-clls (a) Initial blanked cut cell (b) 8 vertex & 8 triangle form of a surface cell (c) Displacement of blanked vertices (d) Calculation of cell area of reformed cut cell

For the structured grid system, a surface cell is typically a square which has 4 vertices. On the 3rd stage, the intersection between Spline boundary and 4 edges of each square surface cell is evaluated. The role of spline boundary information is to cut out blanked area of overlap cell for the cell reconstruction process as represented in Fig. 4-(a). For this process, all the square surface cells are expressed by 8 vertices and 8 triangles for cell deformation by intersection in the Fig. 4-(b). Two vertices are allocated on each vertex of square surface cell and a center point can be evaluated on the averaged point of 4 vertices of the square. Then the eight triangles A-G are generated on the cell. As a matter of course, the area of B, D, F, H is zero. These vertices and triangles are adopted to represent the cell area any deformed surface cell by intersection and to evaluate the cell area of the deformed cell. In Fig. 4-(c), the vertices allocated on the blanked vertex are displaced to the intersection point with spline boundary. Finally, cut cell case 2 can be deformed as like Fig. 4-(d). This figure shows an example of case 2. And the other cases (3~15) can be expressed by adequate movement of blanked vertex to intersection point. This may be easily determined by users on a case-by-case basis.

2.2.2. Addition of Extra Triangles for Error Correction

The deformed cut cell on the curved boundary as like collar-fuselage interface may deteriorate the accuracy of the predicted aerodynamic coefficients because the curved boundary line case as shown in Fig. 5-(a) is not considered in the main cell deformation process. Therefore the area of extra-triangles composed by 2 intersection points and boundary points included inner region the cell should be incorporated as shown in Fig. 5-(b). The area of each triangle can be easily evaluated using the vertex point information. And the area of surface cut-cells can be finally acquired by subtraction or summation of reformed main cell area and extra-triangle area.

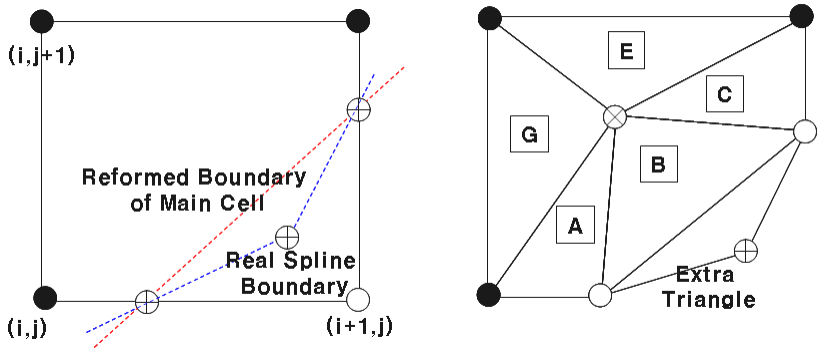

(a) (b)

Fig. 5. Incorporation of Extra-Triangle in Cut-Cells (a) Concave type Spline-boundary (b) Addition of Extra-Triangle

2.2.3. Integration of Aerodynamic Coefficients

On the last sequence, the cell area is calculated by the summation of areas of 8 triangles on each surface cell except blanked cell. In case of hole-cell, the surface cell area is set to 0. And

aerodynamic coefficients are integrated using the evaluated surface cell-area. Surface grid set of DLR-F4 reconstructed by S-BIG scheme is presented in Fig. 6.

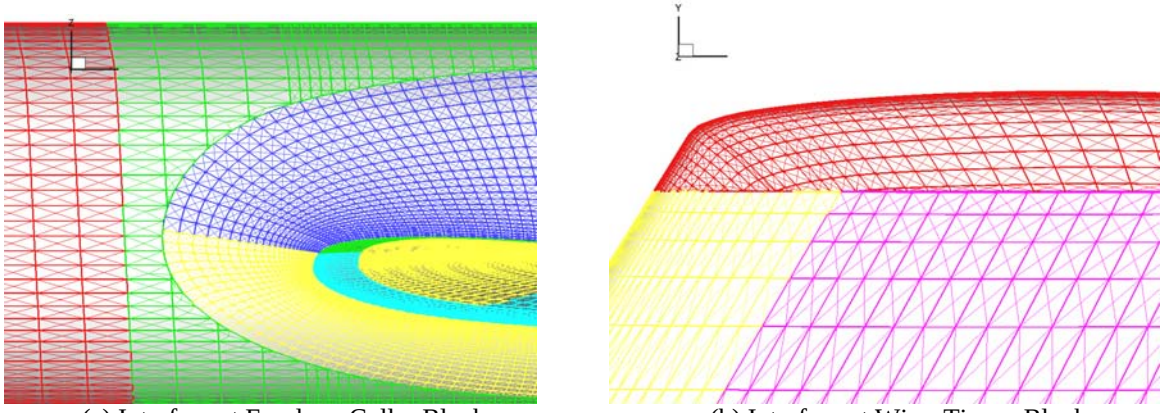

(a) Interface at Fuselage-Collar Blocks (b) Interface at Wing-Tipcap Blocks

Fig. 6. Reconstructed surface grid on DLR-F4 W/B configuration

2.3 Geometric Modification Method for Overlapped Surfaces

With regard to the geometric modification of overlapped surface, a spline function is used for highly flexible surface modification. The most knotty problem is that the overlapped surface at the block to block boundary should be simultaneously modified with an equal deformation. Therefore the surface grids are modified according to the deformation of the Spline patch over the aircraft surface based on mapping from physical grid points to patched function. Figure 7 shows that all the overlapped block surfaces are mapped upon one patched spline. In the present work, geometric modification is limited to wing surface modification in the normal direction for wing planform according to *z*-axis. The mapping procedure is presented as follows.

The spline surface equation is given by Eq. (1).

$$C(u,v)=\sum_{j=0}^{m}\sum_{i=0}^{n}P_{i,j}N_{i,k}(u)N_{j,l}(v)\,, \tag{1}$$

and $P_i=(x_i,y_i,z_i)$ is a position vector of the i^{th} control point in three-dimensional space. The value of *n*, *m* indicates a number of control points on the *u*-, *v*-direction, respectively. And blending functions are defined as

$$N_{i,k}(u)=\frac{(u-t_i)N_{i,k-1}(u)}{t_{i+k-1}-t_i}+\frac{(t_{i+1}-u)N_{i+1,k-1}(u)}{t_{i+k}-t_{i+1}}\,,\quad N_{i,0}(u)=\begin{cases}1 & (t_i\le u\le t_{i+1})\\ 0 & (otherwise)\end{cases}, \tag{2}$$

where $t_i(i=0,1,2,\cdots)$ are knot-values, and subscript *k*, *l* indicates the order of B-spline blending function. This equation is a patched surface on the whole wing surface from wing root to wing tip as shown in Fig. 7-(a).[5]

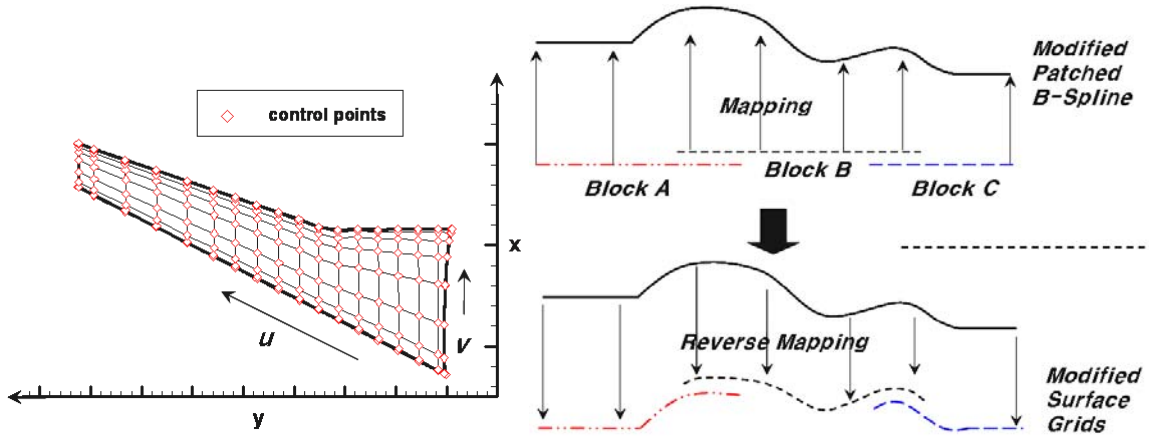

(a) (b)

Fig. 7. Mapping on u-v spline coordinate and surface grid modification (a) Patched B-spline surface and its control points (b) Mapping process from surface grids of overlapped blocks to spline coordinate

The surface grids of collar, wing, tipacp blocks(*x*-*y* plane) are mapped on the *u*-*v* plane of patched surface coordinate by equation (3).

$$C(u,v)=\begin{Bmatrix} x_{surf} \\ y_{surf} \end{Bmatrix}, \tag{3}$$

The *u*-*v* coordinate corresponding to each surface grid is evaluated by Newton Raphson Method. According to the displacement of the design variables (the control points of patched surface), the surface is modified. And the corresponding surface grids are simultaneously deformed following the patched surface. Figure 7-(b) shows a simple 1-D illustration of the surface modification process.

After this process, grid sensitivity for each surface grid $X_{surf}=(x_{surf},y_{surf},z_{surf})$ is finally evaluated as in Eqs. (4).

For the $(i,j)^{th}$ design variable, the grid sensitivity is as follows

$$\frac{\partial X_{surf}}{\partial P_{i,j}}=N_{i,k}(u_{surf})N_{j,l}(v_{surf}), \tag{4}$$

Where (u_{surf},v_{surf}) are the corresponding coordinate on *u*-*v* plane to each surface grid X_{surf}.

2.4 Sensitivity Analysis for Overset Boundary

The formation of discrete adjoint variable method with overset boundary formulations are presented in this chapter. The brief explanation of discrete adjoint variable method is as follows.

The discrete residual of the steady-state flow equations can be written as

$$\{R\}=\{R(Q,X,D)\}=\{0\}, \tag{5}$$

where Q is the flow variable vector, X is the computational grid position and D is the vector of design variables. Similarly, the vector of the aerodynamic objective function F to be

either minimized or maximized is also dependent on Q, X and D as

$$\{F\} = \{F(Q, X, D)\}. \tag{6}$$

The sensitivity derivatives of the aerodynamic function are calculated by directly differentiating Eqs. (5) and (6) with respect to D as

$$\left\{\frac{dR}{dD}\right\} = \left[\frac{\partial R}{\partial Q}\right]\left\{\frac{dQ}{dD}\right\} + \left[\frac{\partial R}{\partial X}\right]\left\{\frac{dX}{dD}\right\} + \left\{\frac{\partial R}{\partial D}\right\} = \{0\}, \tag{7}$$

$$\left\{\frac{dF}{dD}\right\} = \left\{\frac{\partial F}{\partial Q}\right\}^T\left\{\frac{dQ}{dD}\right\} + \left\{\frac{\partial F}{\partial X}\right\}^T\left\{\frac{dX}{dD}\right\} + \left\{\frac{\partial F}{\partial D}\right\}. \tag{8}$$

Efficient evaluation of {dQ/dD} from Eq. (7) is required in problems involving many design variables. In adjoint variable methods, the sensitivity derivatives of the aerodynamic function are obtained by combining Eq. (7) with Eq. (8) as

$$\begin{aligned}\left\{\frac{dF}{dD}\right\} = &\left\{\frac{\partial F}{\partial Q}\right\}^T\left\{\frac{dQ}{dD}\right\} + \left\{\frac{\partial F}{\partial X}\right\}^T\left\{\frac{dX}{dD}\right\} + \left\{\frac{\partial F}{\partial D}\right\} \\ &+ \Lambda^T\left(\left[\frac{\partial R}{\partial Q}\right]\left\{\frac{dQ}{dD}\right\} + \left[\frac{\partial R}{\partial X}\right]\left\{\frac{dX}{dD}\right\} + \left\{\frac{\partial R}{\partial D}\right\}\right),\end{aligned} \tag{9}$$

where Λ represents the 7-element adjoint vector. Rearranging Eq. (9) yields the following equation.

$$\begin{aligned}\left\{\frac{dF}{dD}\right\} = &\left\{\frac{\partial F}{\partial X}\right\}^T\left\{\frac{dX}{dD}\right\} + \left\{\frac{\partial F}{\partial D}\right\} + \Lambda^T\left(\left[\frac{\partial R}{\partial X}\right]\left\{\frac{dX}{dD}\right\} + \left\{\frac{\partial R}{\partial D}\right\}\right) \\ &+ \left(\left\{\frac{\partial F}{\partial Q}\right\}^T + \Lambda^T\left[\frac{\partial R}{\partial Q}\right]\right)\left\{\frac{dQ}{dD}\right\}\end{aligned}. \tag{10}$$

Without the necessity of evaluating the vector {dQ/dD}, the sensitivity derivatives of the aerodynamic function can be calculated as

$$\left\{\frac{dF}{dD}\right\} = \left\{\frac{\partial F}{\partial X}\right\}^T\left\{\frac{dX}{dD}\right\} + \left\{\frac{\partial F}{\partial D}\right\} + \Lambda^T\left(\left[\frac{\partial R}{\partial X}\right]\left\{\frac{dX}{dD}\right\} + \left\{\frac{\partial R}{\partial D}\right\}\right), \tag{11}$$

if and only if the adjoint vector Λ satisfies the following adjoint equation.

$$\left[\frac{\partial R}{\partial Q}\right]^T\Lambda + \left\{\frac{\partial F}{\partial Q}\right\} = \{0\}^T. \tag{12}$$

The solution vector Λ is obtained by solving the Euler implicit method of Eq. (12) time-iteratively as

$$\begin{aligned}\left(\frac{I}{J\Delta t} + \left[\frac{\partial R}{\partial Q}\right]_{VL}^T\right)\Delta\Lambda &= -\left[\frac{\partial R}{\partial Q}\right]^T\Lambda^m - \left\{\frac{\partial F}{\partial Q}\right\}^T, \\ \Lambda^{m+1} &= \Lambda^m + \Delta\Lambda.\end{aligned} \tag{13}$$

The adjoint equation (13) is solved by a time integration scheme with the boundary conditions of Eq. (14), (15).

$$\left[\frac{\partial R}{\partial Q}\right]^T \Lambda + \left[\frac{\partial R_B}{\partial Q}\right]^T \Lambda_B + \left\{\frac{\partial F}{\partial Q}\right\}^T = \{0\}^T , \tag{14}$$

$$\left[\frac{\partial R}{\partial Q_B}\right]^T \Lambda + \left[\frac{\partial R_B}{\partial Q_B}\right]^T \Lambda_B + \left\{\frac{\partial F}{\partial Q}\right\}^T = \{0\}^T . \tag{15}$$

where subscript B reprent boundary cell. In Eq.(15), adjoint variable Λ_B of boundary cell is updated by inner cell-values of n th time step. And the variables of the next time step $(n+1)$ are evaluated by Eq.(14) using the boundary values from (15).

Overset boundary conditions can be derived by a similar way to the conventional adjoint boundary conditions except the number of equations as like Eq. (16)-(19).

$$\left[\frac{\partial R^M}{\partial Q^M}\right]^T \Lambda^M + \left[\frac{\partial R_F^S}{\partial Q^M}\right]^T \Lambda_F^S + \left\{\frac{\partial F^M}{\partial Q^M}\right\}^T = \{0\}^T , \tag{16}$$

$$\left[\frac{\partial R^S}{\partial Q^S}\right]^T \Lambda^S + \left[\frac{\partial R_F^M}{\partial Q^S}\right]^T \Lambda_F^M + \left\{\frac{\partial F^S}{\partial Q^S}\right\}^T = \{0\}^T . \tag{17}$$

$$\left[\frac{\partial R^M}{\partial Q_F^M}\right]^T \Lambda^M + \left[\frac{\partial R_F^M}{\partial Q_F^M}\right]^T \Lambda_F^M + \left\{\frac{\partial F^M}{\partial Q_F^M}\right\}^T = \{0\}^T , \tag{18}$$

$$\left[\frac{\partial R^S}{\partial Q_F^S}\right]^T \Lambda^S + \left[\frac{\partial R_F^S}{\partial Q_F^S}\right]^T \Lambda_F^S + \left\{\frac{\partial F^S}{\partial Q_F^S}\right\}^T = \{0\}^T . \tag{19}$$

where the subscript F represent fringe cells and the superscript M and S represent the main grid and sub-grid domain respectively. Through these 4 system equations, each overset boundary values can be updated to inner adjoint variables of the next time step. Inner values of sub-grid domain are evaluated by Eq. (18), (17) orderly. And for the main-grid domain calculations are carried out from (19) to (16).

3 FLOW ANALYSIS

3.1 Overset Mesh System for a W/B configuration

Large scale computations over wing/body configurations are actively performed centering around ‘Drag Prediction Conference’. In the first drag prediction conference, the provided test geometry of drag prediction is DLR-F4, which consists of wing and fuselage. [2, 13] Figure 8-(a), (b) show the overall mesh system of 7 blocks over DLR-F4. Those 7 blocks are global box, fuselage box, wing box, fuselage grid, collar grid, wing grid, and tip cap grid. Global box is O-type circular grid. And other box grids are Cartesian grids. The total number of mesh points (7 blocks) is about 300 thousands pts. To guarantee a good grid quality, collar grid is positioned at the interface of wing and fuselage and tip cap grid on the wing tip. Fuselage grid is made up of 1 block using untrimmed approach. Orphan cells on the overlapping surfaces are resolved by sub-cell transfinite interpolation developed by Noack et al for N-S design problem. [11] Tip cap grid is made in C-type.

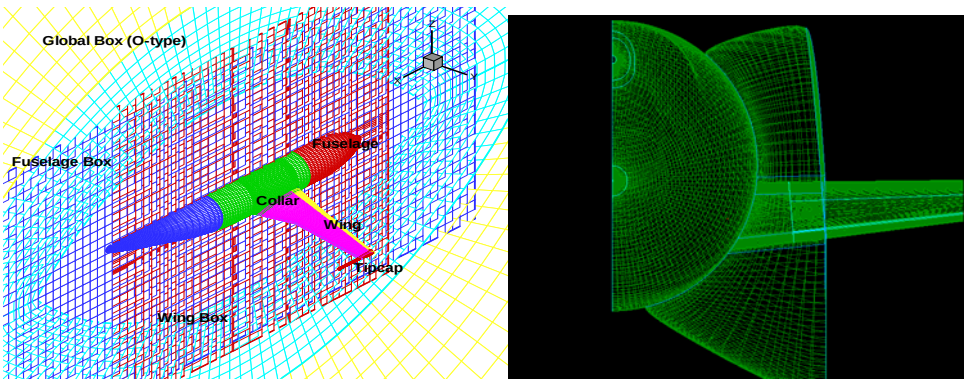

(a) (b)

Fig. 8. Overset mesh system for DLR-F4 (a) Composition of mesh system (b) Collar grid

3.2 Numerical Techniques for Flow Analysis

The governing equations are the three-dimensional compressible Euler equations. The governing equations are transformed in generalized coordinates and are solved with a finite-volume method. For the calculation of residual, convective terms are upwind-differenced based on RoeM scheme by Kim et al. [19]. A MUSCL (Monotone Upstream Centered Scheme for Conservation Laws) approach using a third order interpolation is used to obtain a higher order of spatial accuracy in all calculations. For temporal integration, Yoon's LU-SGS scheme is applied.

3.3 Test Case for Flow Analysis & Design Optimization

The flow conditions for the test case are that free stream Mach number is 0.75 and angle of attack is 0.5 degree. The flow analysis results are presented in Fig. 9. Those show that the block to block interpolation is carried out very well. Weak shock is observed on the upper wing surface and drag minimization will be presented through weakening shock-strength in the next chapter.

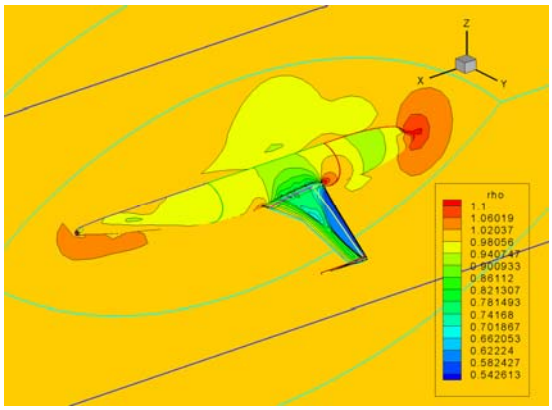

Fig. 9. Flow Analysis Results – Density Contour

4 DESIGN OPTIMIZATION

4.1 Drag Minimization

The presented overset design approach is used for design optimization of W/B configuration. Optimization is performed using the Broydon-Fletcher-Goldfarb-Shanno (BFGS) variable metric method supported by the DOT (Design Optimization Tool) commercial software. 15 arrays of design variables are allocated along the span direction and 7 arrays on the wing cord direction. Totally 105 geometric design variables are given on the upper and lower wing surfaces respectively.

The objective is to minimize drag coefficient with lift constraint. To avoid the necessity of performing the sensitivity analysis twice for lift and drag coefficients, the objective function to be minimized is given by the following equation:

$$F = \omega \times Cd + \max(Cl_0 - Cl, 0.0)\,, \tag{20}$$

where Cl_0 is the target lift coefficient and ω is a weighting value. And the weighting factor is determined by the ratio of sensitivities of drag and lift coefficients for angle of attack.[7] The initial and designed surface pressure coefficients are compared in Fig. 10. After 67 design iterations based on flow solver, the drag coefficient is reduced from 0.0298 to 0.0243 by keeping the target lift coefficient at a threshold value of 0.7622. The shock wave causing wave drag on the initial airfoil is disappeared on the designed airfoil, which is definitely evident in Fig. 10. Through the design results, it is demonstrated that the overset mesh technqiues are adequately adapted to aerodynamic shape optimization problem.

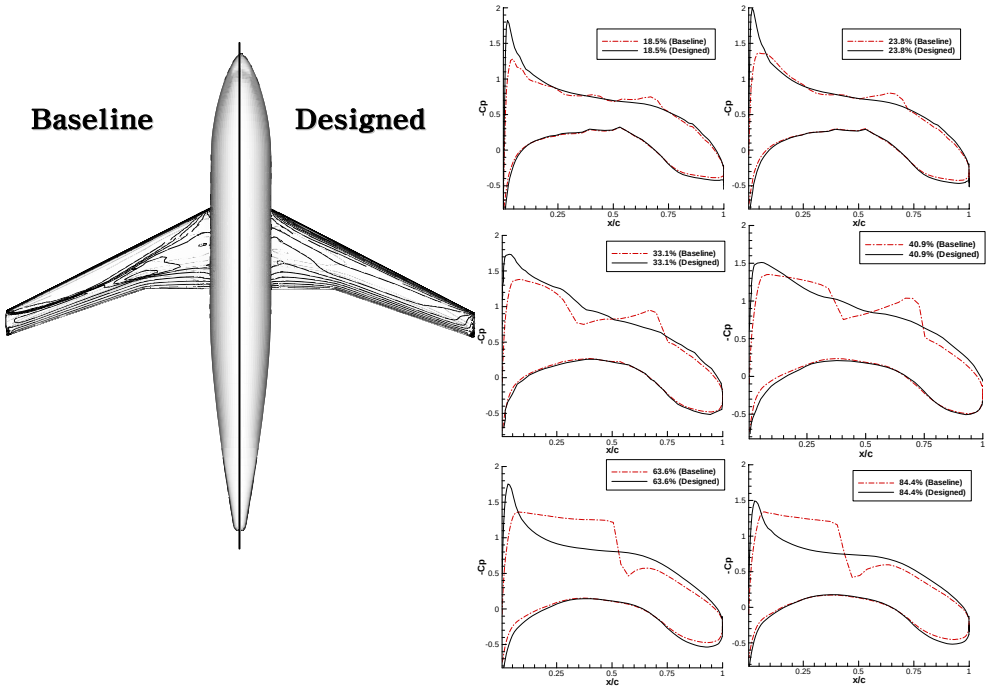

Fig. 10. Drag Minimization of W/B Configurations (Surface Pressure Distributions)

5 CONCLUSIONS

- A new optimal design approach based on overset mesh technique and adjoint formulas. Especially, the overset boundary conditions for discrete adjoint variable method are carefully derived.
- Overset flow analysis techniques are adequately adapted to the sensitivity analysis code and design modules by improvement or development.
- For the pre-processing of the overset flow analysis and sensitivity analysis, finding block connectivity is automatically carried out by overlap optimization. And improvement of convergence characteristics can be achieved in adjoint variable code through the overlap optimization.
- For the post-processing code, the aerodynamic coefficients are evaluated by Spline-Boundary Intersecting Grid Scheme (S-BIG) for convenient calculation of {dF/dQ} term in the sensitivity analysis.
- W.R.T. the grid modification in the design process, the overlapped surfaces of collar, wing, tipcap blocks can be displaced simultaneously by mapping to B-spline patch on the wing surface.
- The present design approach with the special techniques for overset mesh system, successfully demonstrated its capability for the aerodynamic shape optimization of complex geometry design problems.

REFERENCES

[1] William M. Chan, Reynaldo J. Gomez III, Stuart E. Rogers, Pieter G. Buning, “Best Practices in Overset Grid Generation,” AIAA Paper 2002-3191.
[2] C. L. Rumsey, Robert T. Biedron, “Computation of Flow Over a Drag Prediction Workshop Wing/Body Transport Configuration using CFL3D,” NASA TM-2001-211262.
[3] K. Leoviriyakit, S. Kim, and A. Jameson, “Viscous Aerodynamic Shape Design Optimization of Wings including Planform Variables,” AIAA Paper 2003-3498.
[4] S. Choi, J.J. Alonso, S. Kim, I. Kroo, and M. Wintzer, "Two-Level Multi-Fidelity Design Optimization Studies for Supersonic Jets," AIAA Paper 2005-0531.
[5] B.J. Lee, C. Kim, and O. Rho, “Optimal Shape Design of the S-Shaped Subsonic Intake Using NURBS,” AIAA Paper 2005-0455.
[6] E.J. Nielsen, and W.K. Anderson, “Aerodynamic Design Optimization on Unstructured Meshes Using the Navier-Stokes Equations,” AIAA Paper 98-4809.
[7] H.J. Kim, D. Sasaki, S. Obayashi, and K. Nakahashi, “Aerodynamic Optimization of Supersonic Transport Wing Using Unstructured Adjoint Method,” *AIAA J.*, 39(6) (2001) pp.1011-1020.
[8] S. Nadarajah, A. Jameson, "Studies of the Continuous and Discrete Adjoint Approaches to Viscous Automatic Aerodynamic Shape Optimization," AIAA Paper 2001-2530.
[9] C.S. Kim, Chongam Kim, O.H. Rho, “Feasibility Study of Constant Eddy-Viscosity Assumption in Gradient-Based Design Optimization,” J. of Aircraft, 40(6) (2003) pp.1168-1176.
[10] W. Liao, and H.M. Tsai, “Aerodynamic Design Optimization by the Adjoint Equation

Method on Overset Grids," AIAA Paper 2006-54
[11] Ralph W. Noack, and Davy M. Belk, "Improved Interpolation for Viscous Overset Grids," AIAA Paper 97-0199.
[12] Norman E. Suhs, Stuert E. Rogers, and William E. Dietz, " PEGASUS 5: An Automated Pre-processor for Overset-Grid CFD," AIAA Paper 2002-3186.
[13] J. C. Vassberg, P. G. Buning, and C. L. Rumsey, " Drag Prediction for the DLR-F4 Wing /Body using OVERFLOW and CFL3D on an Overset Mesh," AIAA Paper 2002-0840.
[14] R.L. Meakin, "Object X-rays for Cutting Holes in Composite Overset Structured Grids," AIAA Paper 2001-2537.
[15] D.M. Belk, and R.C. Maple, "Automated Assembly of Structured Grids for Moving Body Problems," AIAA Paper 95-1680.
[16] D.L. Brown, W.D. Henshaw, and D.J. Quinlan, "Overture: Object-Oriented Tools for Overset Grid Applications," AIAA Paper 99-3130.
[17] W.M. Chan and P.G. Buning, "Zipper Grids for Force and Moment Computation on Overset Grids," AIAA Paper 95-1681.
[18] Nathan Hariharan, Z.J. Wang, and P.G. Buning, " Application of Conservative Chimera Methodology in Finite Difference Settings," AIAA Paper 97-0627.
[19] Sung-soo Kim, Chongam Kim, Oh-hyun Rho, and Seung Kyu Hong, " Cures for the Shock Instability: Development of Shock-Stable Roe Scheme," *J. of Computational Physics*, 185(2) (2003) pp.342-374.